



Special Feature: Nondestructive Testing and Evaluation Technology

Research Report

Visualization of Surface Cracks and Monitoring of Back-wall Crack Growth via Potential Drop Techniques

Yasumoto Sato, Naomi Kawaguchi, Natsuki Ogura, Tsunaji Kitayama, Akira Ohashi and Yoshihiro Odagiri

Report received on Nov. 4, 2013

■ **ABSTRACT** ■ We have investigated the applicability of potential drop (PD) techniques to the visualization of surface cracks and continuous monitoring of back-wall cracks. An intergranular stress corrosion crack (IGSCC) with complicated surface morphology was selected as a target defect for visualization. Visualization of the IGSCC was performed (measurement of the PD distribution) using the induced current potential drop (ICPD) technique. Lines containing PDs with sudden changes due to the existence of cracks were observed using the PD distributions. The shapes of the lines agree well with those of the main and branched cracks, and therefore, the IGSCC was successfully visualized by the ICPD technique; however, small cracks located near larger cracks were not visualized.

Measurements using the direct current potential drop (DCPD) technique were conducted on the specimen under cyclic loading. The measured potential drop increased as the cyclic loading (number of cycles) increased, and after termination of the cyclic loading, a back-wall crack reached the surface of the specimen between the two potential drop terminals. Accordingly, a back-wall fatigue crack was successfully monitored during cyclic loading using the DCPD technique. The crack growth rate estimated by the DCPD technique was in good agreement with that obtained by the fracture surface observation via scanning electron microscopy. This means that the DCPD technique can precisely detect back-wall crack initiation under cyclic loading.

■ **KEYWORDS** ■ Potential Drop Technique, Visualization, Surface Crack, Monitoring, Back-wall Crack, Fatigue Crack

1. Introduction

Potential drop (PD) techniques utilize an electrical current supplied to the investigated materials and measure the perturbation of the current due to discontinuities in the material, such as cracks and/or changes in the properties of the material. The PD techniques are divided roughly into a direct-current potential drop (DCPD) technique⁽¹⁾ and an alternating-current potential drop (ACPD) technique⁽²⁾ according to the current utilized. In this paper, two application examples of the PD techniques are presented.

For the first case, we investigated the visualization of surface cracks using the induced current potential drop (ICPD) technique. The ICPD technique is a modified version of the ACPD technique for the detection and sizing of defects. Prior to a detailed investigation of a defect in the depth direction, a

surface observation of the defect by microscopy was conducted on a sample cut from a defected portion of a structure when the defect was detected during an in-service inspection that used nondestructive inspection techniques.⁽³⁾ However, surface observation by microscopy requires the investigator to have certain technical skills and is generally a time consuming task. Furthermore, it is sometimes difficult to identify whether a defect, such as a mark observed on a specimen by microscopy, is a harmful defect (e.g., a crack) or a harmless scratch mark. Therefore, an effective method that allows a detailed visualization of defects is required to support surface observations by microscopy. The method should be able to identify small defects and should be an automated procedure. The ICPD technique, based on electromagnetic induction, has been developed⁽⁴⁾ to overcome the difficulty of defect detection when using the conventional PD techniques, which utilize electrical

terminals that are connected to the measured material. The applicability of the ICPD technique for the detection of small cracks⁽⁵⁻⁷⁾ and the sizing of fatigue cracks^(8,9) has been demonstrated. Cracks investigated in these previous studies are mainly single fatigue cracks, and the applicability of the ICPD technique to detect/visualize multiple cracks that are closely located to each other and/or branched cracks, such as intergranular stress corrosion cracks, have not been investigated. The ICPD technique measures PDs on the surface of the material using a pair of needle probes, and thus a high spatial resolution can be obtained. Considering the above mentioned applications to single cracks and the high spatial resolution, the ICPD technique has a potential to visualize multiple and/or branched surface cracks with high sensitivity and high spatial resolution.

For the second case, we monitored back-wall fatigue cracks in a welded region using the DCPD technique. Monitoring a material continuously under a dynamic loading condition can result in an improved reliability of the components/systems, and the optimization of the fatigue test, which is generally a time consuming task, can be achieved because the rate of the continuous crack growth will be known due to the continuous monitoring of the specimen. The techniques that are employed for the continuous monitoring of materials should be reliable, accurate, sensitive, and simple. The DCPD technique is not suitable to detect defects because current supply terminals must be connected to the material in order to supply a constant current. On the other hand, the DCPD technique is suitable to continuously monitor various components, structures, and specimens since the technique utilizes a very simple sensor, which merely consists of electrical wiring, and measured data can be recorded continuously and easily.

2. Visualization of Surface Cracks via the ICPD Technique

2.1 ICPD Technique

2.1.1 Principle of the ICPD Technique

When a coil that has an alternating current is located near conductive materials, an electrical current is induced due to electromagnetic induction. The ICPD technique measures the PD caused by the perturbation of the induced current that occurs as a result of defects.

The ICPD technique uses a coil as an exciter, which is positioned 40 mm away from the surface of the conductive material that is inspected. The influence of the surface irregularity of the material on the measured PD is considered to be relatively small and the scattering superposed on the measured PD can be reduced. **Figure 1** shows a schematic illustration of the ICPD sensor used in this study.

2.1.2 PD Distribution around Surface Cracks

Figure 2 shows a schematic of a PD distribution, which will be obtained by the ICPD technique around a surface crack, along with illustrations of an induced current density distribution and the location of the PD pick-up pins of the sensor. The figure is drawn according to the interpretations of a PD distribution for

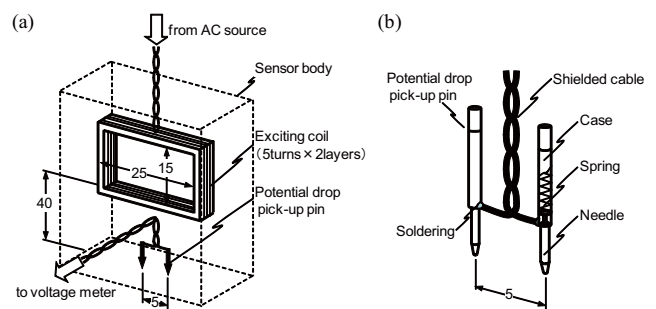


Fig. 1 Schematic illustration of the sensor for ICPD technique, (a) whole view and (b) detail of the potential drop pick-up pins.

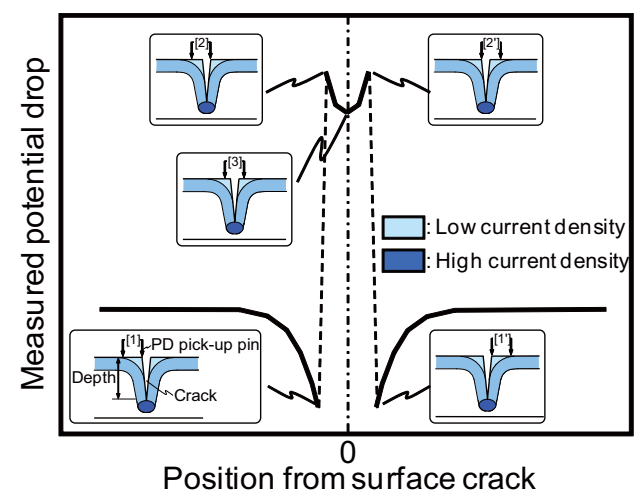


Fig. 2 Schematic illustration of a potential drop distribution measured around a surface crack.

a surface crack.⁽¹⁰⁾ For surface cracks, the PD distribution is complex around the crack. The measured PD decreases as the sensor moves toward the crack until one of the PD pick-up pins becomes located next to the crack due to the low current density region at the edge of the crack (position [1] in Fig. 2). The PD increases when one of the PD pick-up pins crosses the crack, since the length of the induced current path increased (position [2] in Fig. 2). The PD distribution measured while the PD pick-up pins were across the crack is a “U” shape due to changes in the effect of the low current density region between the PD pick-up pins on the measured PD. Accordingly, when a line of measurement is on a single crack, there will be a pair of sensor positions where the PD shows a sudden change within the distance between the two PD pick-up pins of the sensor.

2.2 Experimental Setup

2.2.1 Specimen

In order to demonstrate the applicability of the ICPD technique to the visualization of surface cracks, we selected an intergranular stress corrosion crack (IGSCC) as the target crack for the visualization. An IGSCC sometimes shows complicated surface morphology, and is therefore suitable to show the visualization capability of the ICPD technique.

A plate specimen (218 mm × 100 mm × 10 mm) was machined from type 316 stainless steel and a simulated IGSCC was introduced into the specimen under a magnesium chloride solution. The crack was located around the center of the cracked surface of the specimen.

2.2.2 ICPD Measurement Procedure

As shown in Fig. 3, an XY coordinate system was introduced on the cracked surface of the specimen. The origin of the coordinate system was set at the center of the cracked surface and the X axis was aligned to be parallel to the longitudinal direction of the specimen. Measurement lines were set at even intervals parallel to the X axis, since the crack was introduced in the Y direction. Measurements were performed using the sensor to scan along the measurement line with the longest edge of the exciting coil aligned with the measurement line. The measuring system was completely automated and used a computer-controlled

XYZ stage to perform the automated scans of the sensor. The measurement range and intervals are summarized in Table 1.

The alternating current supplied to the exciting coil of the sensor was set to 10 kHz and 3 A, which were determined to be the optimized values for surface cracks when using a specimen with artificial cracks prior to the experiment.

2.3 Results and Discussion

The visualization results (PD distribution obtained around the IGSCC) and a photo of the measured area of the specimen are shown in Fig. 4. According to Fig. 4(a), the measured PDs show a symmetric distribution for $X = 0$. This is due to the fact that the sensor is symmetrically shaped and only a pair of PDs for a single crack was measured. In order to correlate the PD distribution with the photo of the measured area, the $-X$ region of the PD distribution is shaded in Fig. 4(a). As can be seen in Fig. 4(a), the curves of the gray lines, which correspond to the PDs that changed suddenly for each measurement line, agree well with those of the main and branched cracks shown in the photo of the measured area. Furthermore, PD changes generated by the existence of subcracks 1-3 can also be observed. On the other hand, PD changes for

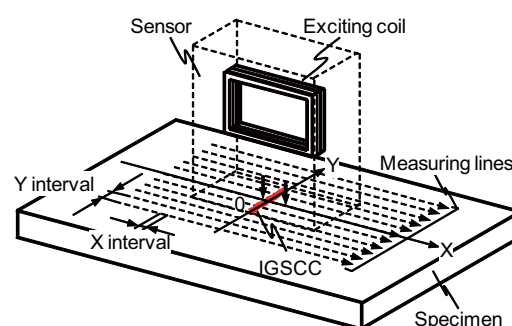


Fig. 3 Illustrations of a plate specimen with a crack, measuring lines and the sensor for the ICPD technique.

Table 1 Measurement range and intervals.

	X direction (mm)	Y direction (mm)
Range	-5 ~ 5	-4.6 ~ -13
Interval	0.1	0.4

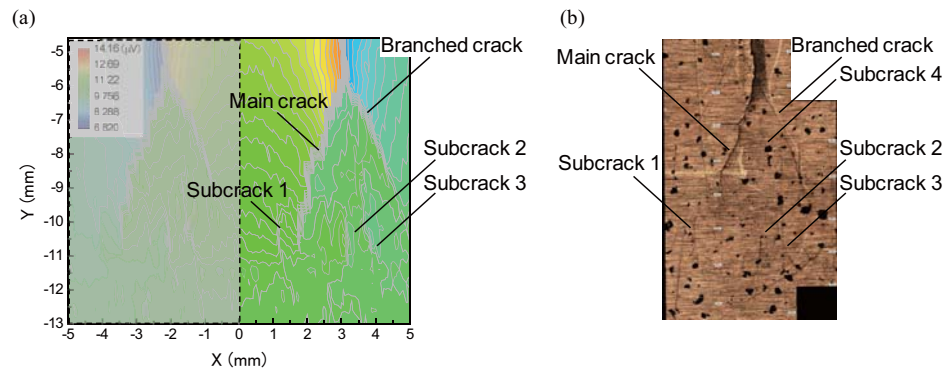


Fig. 4 Visualization results, (a) the measured potential drop distribution and (b) a photo of the measured area.

subcrack 4 are not clear in the corresponding locations on the plot of the PD distribution. According to Fig. 4(b), subcrack 4 is located between the main and branched cracks and its size is smaller than that of the main and branched cracks; therefore, changes in the PD due to subcrack 4 are hidden by those caused by the main and branched cracks.

Accordingly, although small cracks located near large cracks are not be visualized, an automated visualization of the surface cracks can be performed by using the ICPD technique with a computer-controlled XYZ stage.

3. Monitoring of a Back-wall Crack via the DCPD Technique

3.1 DCPD Technique

The DCPD technique utilizes a constant direct current supplied to a material through electrical terminals connected to the material. Potential drops are measured using two electrical terminals connected to the material between the two current supply terminals. A schematic illustration of the PD distribution around a back-wall crack using the DCPD technique is shown in Fig. 5, along with illustrations of the direct current paths around the back-wall crack. When a crack initiation occurs between the two PD terminals, local electrical resistance of the material increases due to a decrease in the cross-sectional area of the current path, and as a result, the PD increases. The PD continuously increases as the back-wall crack depth increases (crack propagation) because the cross-sectional area of the current path continuously decreases with the crack propagation.

3.2 Experimental Setup

3.2.1 Fatigue Test

The materials consisted of flat and L-shaped plates of aluminized steel with a thickness of 0.8 mm. The specimen for the fatigue test was fabricated by seam welding these flat and L-shaped plates together. A schematic illustration of the specimen for the fatigue test is shown in Fig. 6. The specimen was set to a fatigue loading machine using the three bolt holes. The specimen was subjected to load-controlled fatigue at room temperature with a hydraulic servo type material testing machine. The cyclic load was applied to the specimen through bolt hole 1 shown in Fig. 6. The maximum and minimum loads were set at 176.4 N and -19.6 N, respectively. The loading frequency was 5 Hz.

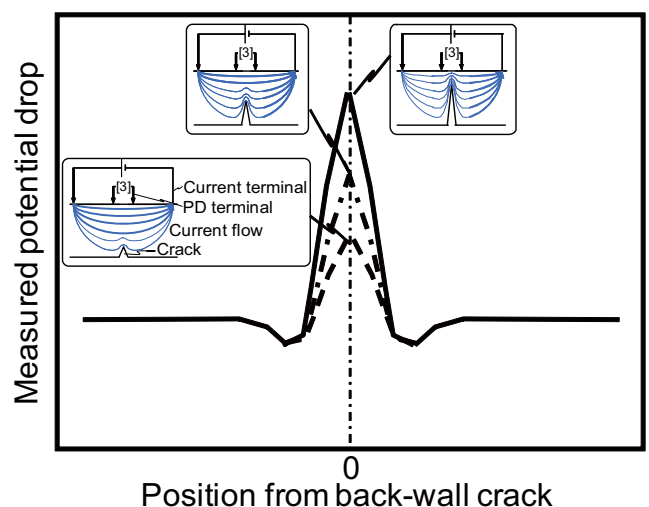


Fig. 5 Schematic illustration of a potential drop distribution measured around a back-wall crack.

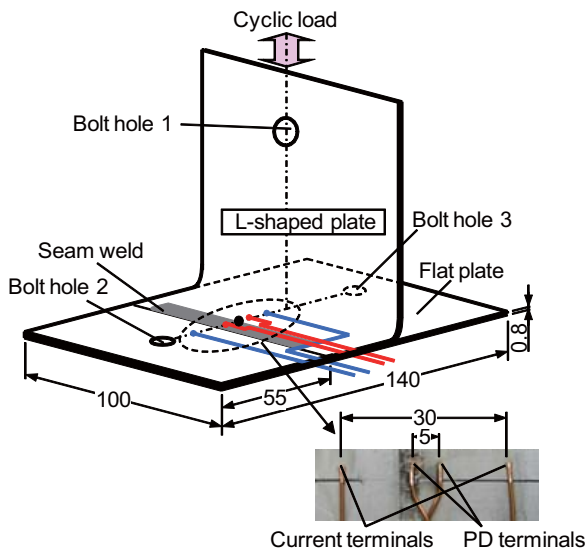


Fig. 6 Schematic illustration of the specimen for the fatigue test.

3.2.2 DCPD Measurement Procedure

Considering the specimen shape and the loading direction shown in Fig. 6, the initiation of the fatigue crack was expected to be on the back-wall of the L-shaped plate at the boundary between the seam weld and the parent material (indicated in Fig. 6 by the black filled circle). Therefore, one of the PD terminals was welded onto the center of the seam weld and the other was welded onto 5 mm away from the previous one using a small spot-welding machine. The two current terminals were welded onto the specimen 30 mm apart.

During the fatigue test, a direct current of 4.0 A was supplied to the specimen through the current terminals and the measured PD using the PD terminals was recorded every 0.5 second. In order to reduce the effect

of joule heating, the current was supplied and stopped every 2.0 seconds.

3.3 Results and Discussion

3.3.1 Continuous Monitoring of a Fatigue Crack Using the DCPD Technique

The PD data that were measured during the fatigue test were processed according to the procedures summarized in **Table 2**.

Figure 7 shows the PD ratio, V/V_0 , measured during the fatigue test. The PD ratio is a value of unity until the loading cycle of 3.00×10^5 . This suggests that no crack initiation occurred or there was a crack with a depth smaller than the detection limit of our DCPD measurement system. After a loading cycle of 3.00×10^5 , the PD ratio increases until the cyclic loading is terminated. After the termination of the cyclic loading, a fatigue crack that reached to the surface of the specimen was visually observed between the two PD terminals. Therefore, the increase in the PD ratio can be attributed to the propagation of the back-wall fatigue crack.

According to the results presented above, one can monitor the cracking behavior of the specimen under a cyclic loading condition using the DCPD technique.

3.3.2 Estimation of the Crack Growth Rate of the Back-wall Fatigue Crack Using the DCPD Technique

The crack growth rate was estimated to be 1.70×10^{-5} mm/cycle when using the PD ratio shown in Fig. 7 and by using the following two assumptions:

Table 2 Data process procedures for the PD measured during the fatigue test.

No.	Process	Output
1	Differentiate the PD of 4 A from that of 0 A	V_{4A} V_{0A}
2	Calculate average V_{4A} and V_{0A} for every 1000 loading cycles	$V_{4A}^{Avg.}$ $V_{0A}^{Avg.}$
3	Calculate $V = V_{4A}^{Avg.} - V_{0A}^{Avg.}$ to reduce the effect of changes in temperature of the specimen	V
4	Extract flat portion from V plotted as function of loading cycle, and calculate the average V_0	V_0
5	Calculate the ratio of V to V_0	V/V_0

Crack initiation occurs when the PD ratio starts to increase (at 3.00×10^5 cycles in Fig. 7).

A crack reaches the surface of the specimen when the cyclic loading is terminated.

According to Fig. 7, although the actual crack growth rate seemed to increase as the loading cycle increased, the estimated crack growth rate was an average value of one. Furthermore, an evaluation of the validity of the two assumptions is required to evaluate the estimated crack growth rate. In the following section, the evaluation of the estimated crack growth rate is described based on a fracture surface observation conducted via scanning electron microscopy (SEM).

3.3.3 Evaluation of the Crack Growth Rate Based on a Fracture Surface Observation

A fracture surface observation was made via SEM. **Figure 8** shows an SEM image obtained for the thickness of the central portion of the specimen, as a typical example of the fracture surface morphology of

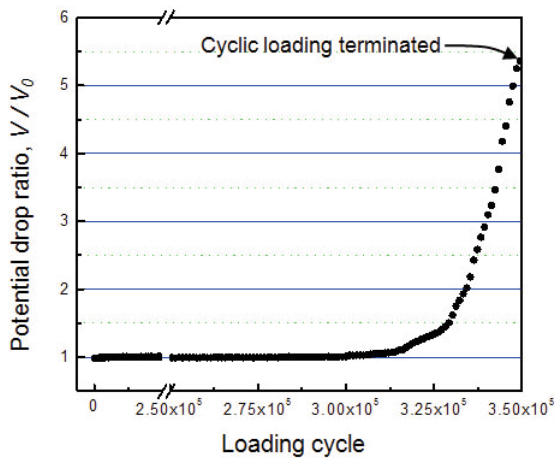


Fig. 7 PD ratio measured during the fatigue test.

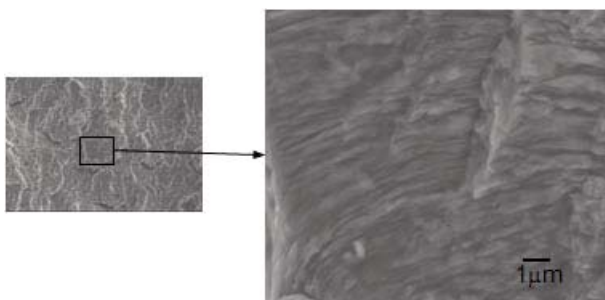


Fig. 8 SEM image obtained for the thickness of the central portion of the specimen.

the specimen. As seen in this figure, striations appear on the specimen as evenly spaced parallel lines. Each striation is actually a shallow crack that results from cyclic loading. The cyclic loading produces an advancing repetition of shallow cracks. Therefore, a crack growth rate can be obtained by measuring the interval of the observed striations. In accordance to Fig. 8, the average crack growth rate within the magnified image was calculated to be 1.54×10^{-5} mm/cycle.

As described in a previous section, the estimated crack growth rate using our DCPD measurement system was 1.70×10^{-5} mm/cycle, which is in good agreement with that obtained by the fracture surface observation. This indicates that the two assumptions for the estimation of the crack growth rate using the DCPD technique are valid. Furthermore, it is confirmed that our DCPD measurement system can precisely detect back-wall crack initiation under cyclic loading.

4. Conclusion

Two kinds of potential drop techniques, namely, the ICPD and DCPD techniques, were introduced for the visualization of a surface crack and monitoring the growth of a back-wall crack, respectively.

For the visualization of a surface crack when using the ICPD technique, an IGSCC with a complicated surface morphology was investigated. The curves of the gray lines in the plot of the PD distribution around the IGSCC agree well with those of the main and branched cracks shown in the photo of the measured area. The gray lines in the plot of the PD distribution correspond to the sudden change in the PD due to the existence of a crack for each measurement line. However, some small cracks located near larger cracks can not be visualized since the corresponding PD changes were hidden by those of the larger cracks.

For monitoring the growth of a back-wall crack while using the DCPD technique, PDs on a back-wall fatigue crack were continuously measured during cyclic loading. The PD measured during the fatigue test increased as the number of loading cycles increased. The estimated crack growth rate obtained when using the DCPD technique agrees well with that obtained by the fracture surface observation. Accordingly, our DCPD measurement system can precisely detect back-wall crack initiation under cyclic loading.

References

- (1) Kanoh, Y. and Abe, H., "Proposal for Nondestructive Evaluation Procedure of 3D Crack Shape by Means of Electrical Potential Method", Transactions of Japan Society of Mechanical Engineers A (in Japanese), Vol. 58, No. 547 (1992), pp. 412-419.
- (2) Collins, R., Michael, D. H. and Clark, R., "Measurement of Crack Depth in a Transition Weld Using ACPD", Review in Progress of Quantitative Nondestructive Evaluation, Vol. 11 (1992), pp. 545-552.
- (3) Okumura, Y., Sakashita, A., Fukuda, T., Yamashita, H. and Futami, Y., "Latest SCC Issues of Core Shroud and Recirculation Piping in Japanese BWRs", Transactions of the 17th International Conference on Structural Mechanics in Reactor Technology (2003), Paper No. WG01-1, IASMiRT.
- (4) Kim, H. and Shoji, T., "A Study on Induced Current Focusing Potential Drop (ICFPD) Technique: Examination of the Sizing Accuracy of Defects and Its Frequency Dependence", Journal of the Society of Materials Science, Japan (in Japanese), Vol. 43, No. 494 (1994), pp. 1482-1488.
- (5) Sato, Y., Takeda, Y. and Shoji, T., "Nondestructive Evaluation of Fatigue and Creep-fatigue Damage by Means of the Induced Current Potential Drop Technique", Fatigue and Fracture of Engineering Materials and Structures, Vol. 24, No. 12 (2001), pp. 885-893.
- (6) Yamashita, M., Tada, S., Sato, Y. and Shoji, T., "Nondestructive Evaluation of Fatigue and Creep-fatigue Damage in 12%Cr Stainless Steel by the Induced Current Focusing Potential Drop Technique", Journal of Testing and Evaluation, Vol. 29, No. 6 (2001), pp. 544-555.
- (7) Sato, Y., Atsumi, T. and Shoji, T., "Application of Induced Current Potential Drop Technique for Measurements of Cracks on Internal Wall of Tube-shaped Specimens", NDT & E International, Vol. 40, No. 7 (2007), pp. 497-504.
- (8) Yi, Y. and Shoji, T., "Measurement of Shape of 3-dimensional Surface Crack Using ICFPD Technique", Transactions of Japan Society of Mechanical Engineers A (in Japanese), Vol. 63, No. 605 (1997), pp. 68-72.
- (9) Sato, Y. and Shoji, T., "Evaluation of Back-wall Fatigue Cracks by Means of Remotely Induced Current Potential Drop Technique and Its FEM Simulation", Transactions of Japan Society of Mechanical Engineers. A (in Japanese), Vol. 72, No. 724 (2006), pp. 1949-1954.
- (10) Sato, Y. and Kim, H., "Detection and Sizing of Cracks Using Potential Drop Techniques Based on Electromagnetic Induction", E-Journal of Advanced Maintenance, Vol. 3, No. 1 (2011), pp. 39-53.

Figs. 1, 3 and 4

Reprinted from NDT & E International, Vol. 49 (2012), pp. 83-89, Sato, Y., Kawaguchi, N., Ogura, N. and Kitayama, T., Automated Visualization of Surface Morphology of Cracks by Means of Induced Current Potential Drop Technique, © 2012 Elsevier, with permission from Elsevier.

Yasumoto Sato

Research Field:

- Development of Nondestructive Inspection Methodology Based on Electromagnetic Phenomena

Academic Degree: Dr.Eng.

Award:

- The Japanese Society for Non-destructive Inspection, Rising Researchers Award, 1998



Naomi Kawaguchi

Research Field:

- Development of Electro Mechanical Systems



Natsuki Ogura

Research Field:

- Development of Nondestructive Inspection Methodology Based on Electromagnetic Phenomena



Tsunaji Kitayama

Research Field:

- Development of Nondestructive Inspection Methodology

Academic Societies:

- Society of Automotive Engineers of Japan
- The Japanese Society for Non-destructive Inspection



Akira Ohashi *

Research Field:

- Reliability Evaluation of Vehicles



Yoshihiro Odagiri *

Research Field:

- Reliability Evaluation of Special Purpose Vehicles



* TOYOTA AUTO BODY CO., LTD.